

An Innovative Power Module with Power-System-In-Inductor Structure

Laili Wang and Doug Malcolm
Sumida Technologies Inc.
Sumida Corporation
Kingston, Canada
laili_wang@us.sumida.com

Yan-Fei Liu Fellow IEEE
Department of Electrical and Computer Engineering
Queen's University
Kingston, Canada
yanfei.liu@queensu.ca

Abstract— This paper presents an integrated power module with the features of high power density and high efficiency. A multi-functional integrated magnetic component is designed. The component has the roles of both the filter inductor and the case of the whole power module. With the assist of finite element analysis (FEA), design and optimization of the proposed inductor are demonstrated. It has higher inductance value than the inductor used in conventional designs. It has bigger coil winding and larger surface area, leading to lower DCR and better thermal performances than plastic packaging. Benefiting from these advantages, the power module constructed based on the inductor can achieve higher efficiency and lower temperature than those based on traditional plastic packaging solutions. Design of the inductor is demonstrated through the combination of analytical and simulation methods. An inductor prototype is built and used in an integrated power module to do experimental tests. Loss breakdown of the power module is executed to show the loss of the magnetic component. The proposed power module shows better performances than the plastic packaging solution.

Keywords—power-system-in-inductor packaging; magnetic performance; inductor design; thermal;

I. INTRODUCTION

Power modules have been widely used in telecom equipment, computer servers, and consumer electronics to provide an integrated solution of power management. In a small package, the power modules should integrate all the functions of their counterparts designed with discrete components so that the system design engineers do not need to spend too much time on the power supply solution, saving time for products development. Besides, integrated power module has better performance than the solution of discrete components in terms of reliability and space saving. Non-isolated step-down power modules are the most popular power modules used in today's industry. They are composed of an integrated buck regulator (or controller with two Mosfets), an inductor, some input and output capacitors, and some auxiliary components.

Figure 1 shows the schematic of a step-down power module. There are quite a few literatures discussing about the

package of high density power modules [1-15]. Embedding magnetics and capacitors in the printed circuit boards is demonstrated in [1], however, core loss of the embedded magnetic material is significant. Low temperature co-fired ceramic (LTCC) technology becomes very popular recently in research and can achieve very high power density [2-4, 8-15]. Micro-inductor and micro-transformer based on thin film technology is another key technology used for power modules [5-7]. The disadvantage of this technology is that it has higher Direct Current Resistance (DCR) and causes more loss than conventional inductors. In industry, there are two typical packaging solutions for making the power modules. One is based on PCB substrate. The regulator die, chip inductor and other parts are soldered or wire-bonded on the substrate, and the whole substrate is packaged using injection molding. Manufacturers, such as Linear uses this technology. The other one is based on lead frame. In this way, all the components are connected to the lead frame through wire-bonding, and the whole module is then packaged with injection molding. TI, Micrel, and Intersil use this technology to package their modules. No matter which technology is employed to package the module, the chip inductor is a necessary part in a power module. And to leave some space for plastic material, the chip inductor should be smaller than the mold. It generally takes up about 1/4~1/3 of the whole volume of the module. This paper proposes a new packaging technology called power-system-in-inductor (PSI²). A customized magnetic component is designed, acting as both the case of the whole power module and the filter inductor of the converter. Section II of the paper presents the structure of the power module; Section III will demonstrate design of the customized inductor based on the combination of analytical and simulation methods. Section IV will build a prototype and do comparison experiments with plastic packaging solution. Section V concludes the paper.

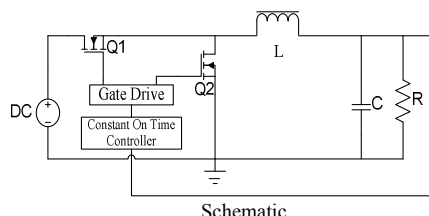


Figure 1. Schematic of a step-down power module.

II. PRINCIPLE OF STRUCTURE

This section will introduce the structure of the proposed power module. A structure based on traditional packaging technology will also be introduced with the purpose of comparison. Power modules in the market are generally packaged with plastic material by injection molding process. Figure 2 shows the structure of the traditional plastic packaging power module. It has a regulator (in the monolithic version) or several active devices (including a controller and two discrete Mosfets in the multiple chips version), an inductor, and some auxiliary components mounted on the substrate together, then the whole substrate is packaged with plastic material. Figure 3 shows the structure of the proposed power module. The proposed structure has a regulator and some auxiliary components, and an inductor mounted on the PCB board. In contrast to conventional plastic packaged power modules, the inductor also acts as a package case of the whole converter. The magnetic core has a cavity in one half and an embedded coil in the other half. The buck regulator and the auxiliary components are embedded underneath the cavity. Thermally conductive glue is used to attach the top of the regulator to the ceiling of the cavity with the purpose of transferring heat from the regulator to the magnetic core. The embedded coil forms an inductor together with the magnetic core. Therefore, the magnetic core has functions of both power module package and filter inductor in the converter. Benefiting from this package technology, the proposed converter has two advantages over the power modules based on conventional plastic package technology. Firstly, without the necessity of leaving enough room for plastic packaging, the inductor size

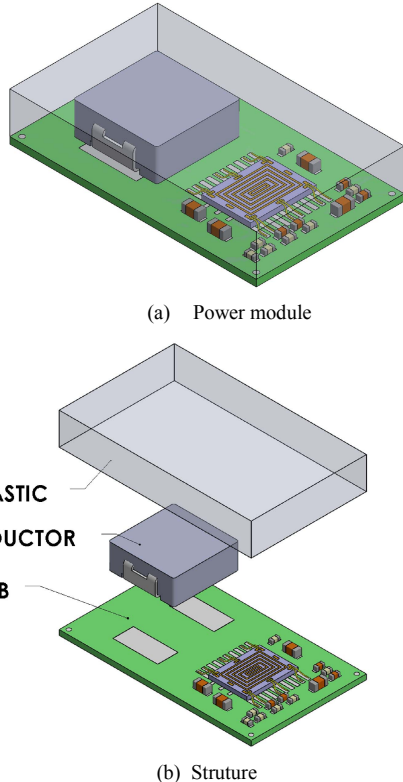
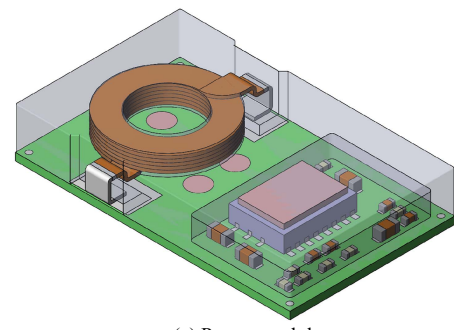
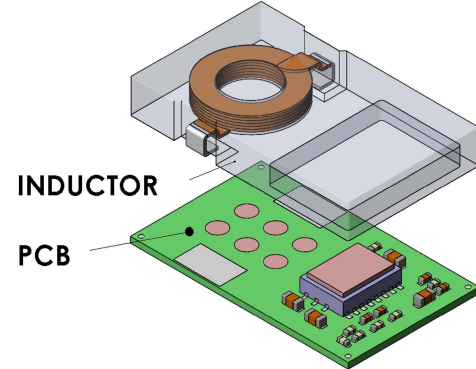


Figure 2. Conventional plastic packing.



(a) Power module



(b) Structure

Figure 3. Proposed magnetic packaging.

could be as big as the package size, which means both the winding and magnetic core will be bigger than those of the inductors used in plastic packing. Compared with a conventional plastic packaged power module with a small metal composite inductor inside, the proposed magnetic packaged power module has lower DCR, higher inductance value since the volume of the inductor is larger. Secondly, in the power module, the heat sources are the semiconductor devices and the inductor. In a plastic packing power module, the heat sources are packaged by the plastic surface (generally 1mm thick), which increases the thermal resistance from the heat sources to ambient. Moreover, the proposed power module has the package composed of magnetic material with higher thermal conductivity than plastic material. It means the magnetic core has better thermal co-efficient and thus lower temperature, which will in turn improve the performance of the whole power module.

III. INDUCTOR DESIGN AND ANALYSIS

There are quite a few literature [9-10, 13-18] discussing about the model of inductance calculation and design. Most of them are for inductors on the semiconductor or PCB, which are not suitable for inductor design in this paper. Since the magnetic core has a customized shape, and there's no existing models for calculating the inductance value, finite element analysis (FEA) is used to simulate the inductance value accurately and design the power module. Benefiting from the proposed structure, the proposed inductor has the same width as the module itself. Therefore, the proposed inductor size is 9mm×9mm×2.8mm. However, the metal powder composite inductor designed for the plastic packaging has to be smaller

than the module to leave enough room for plastic packaging. Generally, the thickness of the plastic layer is around 1mm for thick power modules. Thus the maximum inductor size is 6mm×6mm×1.8mm by considering the extended soldering points on the inductor leads. This Section analyzes the relationship between the inductance L , coil radius R , coil width w , and wire thickness t based on 15mm×9mm×2.8mm package size chosen for prototype demonstration. After a rough calculation to obtain the number of turns, a 3D FEA simulation is used to optimize the inductance and resistance by sweeping parameters above, based on which further analysis and optimization are executed.

Before the simulation, a rough calculation is executed to obtain the possible number of turns based on the initial winding dimension. Figure 4 shows the top view of the winding embedded in the magnetic core. A_s and A_e show the areas of magnetic materials through which the flux lines go. To guarantee the mechanical stress of the iron powder at the inductor terminal (the coil has to be bended), the iron power thickness from the winding coil to the edge of the magnetic core should be large enough, which might results in A_s being larger than A_e . However, they are assumed equal to simplify the design process of the magnetic path when calculating the number of turns. The inductance value calculating equation is expressed in

$$L = \frac{\mu_r \mu_0 N^2 A_e}{l} \quad (1)$$

Where A_e is the effective area for flux density; l is the length of magnetic path; N is the number of turns, μ_r is the relative permeability of the magnetic material. Both A_e and l highly depend on the radius R , width w and thickness t of the coil. The effective area A_e can be calculated by (2)

$$A_e = \pi \cdot r^2 \quad (2)$$

The estimated magnetic path length can be calculated through (3)

$$l = 2h + 2w + r \quad (3)$$

Where h is the total thickness of the winding, and it can be expressed by the height of the inductor H and thickness of magnetic material above or below the winding e in (4)

$$h = H - 2e \quad (4)$$

Substitute (2), (3) and (4) in (1), yielding (5)

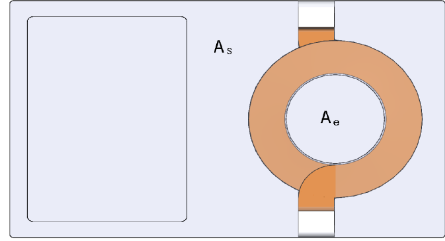


Figure 4. Dimension of the winding.

$$N = \sqrt{\frac{L(2(H-2e) + 2w + r)}{2\mu_r \mu_0 \pi^2}} \quad (5)$$

In this design, the total height of the inductor H is 2.4mm; thickness of magnetic materials above and below the winding e is set to be 0.65 mm in turn number calculation; the relative permeability of the magnetic material μ_r is 10 and the proposed inductance value is 1μH. Number of turns is calculated by substituting these parameters into (5) and sweeping internal radius r and conductor width w . TABLE 1 shows the calculated results. The number of turns increases with the decrease of the internal radius r and increases with the width of the coil w . For the proposed inductor in this paper, the number of turns should include a half turn since it has two terminals leading out from two sides. Therefore, the calculated number of turns should be modified to number of turns in a practical design as shown in TABLE 2. Inductance value calculated based on the TABLE 2 is still close to 1μH although there should be some variations. Based on the calculation and modification, the number of turns can be 3.5, 4.5, 5.5, 6.5, 7.5, 8.5, 9.5 and 10.5 depending on the internal radius and coil width. Even with a simulation tool, it is still very time-consuming to simulate every case of turns. Some of the cases can be easily excluded because of their higher DCR. The equation of DCR calculation is shown in (6):

$$R_{DC} = \rho \frac{2\pi N \cdot (r + \frac{w}{2})}{(\frac{H-2e}{[N]} - s) \cdot w} \quad (6)$$

Where N is the number of turns listed in TABLE 2; ρ is the resistivity of the copper; s is the thickness of the insulation layer; $[N]$ is the ceiling integral of the calculated turns listed in TABLE 1.

TABLE 1 CAUCULATED NUMBER OF TURNS FOR THE PROPOSED INDUCTOR

| w (mm) | 1.00 | 1.20 | 1.40 | 1.60 | 1.80 | 2.00 | 2.20 | 2.40 | 2.60 | 2.80 | 3.00 |
|---------------|-------------|-------------|-------------|-------------|-------------|-------------|-------------|-------------|-------------|-------------|-------------|
| r (mm) | 8.1 | 8.4 | 8.7 | 9.0 | 9.3 | 9.6 | 9.8 | 10.1 | 10.3 | 10.6 | 10.8 |
| 1.00 | 6.6 | 6.9 | 7.1 | 7.3 | 7.6 | 7.8 | 8.0 | 8.2 | 8.4 | 8.6 | 8.8 |
| 1.25 | 5.7 | 5.9 | 6.1 | 6.2 | 6.4 | 6.6 | 6.8 | 6.9 | 7.1 | 7.2 | 7.4 |
| 1.50 | 5.0 | 5.1 | 5.3 | 5.4 | 5.6 | 5.7 | 5.9 | 6.0 | 6.2 | 6.3 | 6.4 |
| 1.75 | 4.4 | 4.6 | 4.7 | 4.8 | 5.0 | 5.1 | 5.2 | 5.3 | 5.5 | 5.6 | 5.7 |
| 2.00 | 4.0 | 4.1 | 4.3 | 4.4 | 4.5 | 4.6 | 4.7 | 4.8 | 4.9 | 5.0 | 5.1 |
| 2.25 | 3.7 | 3.8 | 3.9 | 4.0 | 4.1 | 4.2 | 4.3 | 4.4 | 4.5 | 4.6 | 4.7 |
| 2.50 | 3.4 | 3.5 | 3.6 | 3.7 | 3.8 | 3.9 | 4.0 | 4.0 | 4.1 | 4.2 | 4.3 |
| 2.75 | 3.2 | 3.3 | 3.4 | 3.4 | 3.5 | 3.6 | 3.7 | 3.8 | 3.8 | 3.9 | 4.0 |

TABLE 2 PRACTICAL DESIGN NUMBER OF TURNS FOR THE PROPOSED INDUCTOR

| w (mm)\r (mm) | 1.00 | 1.20 | 1.40 | 1.60 | 1.80 | 2.00 | 2.20 | 2.40 | 2.60 | 2.80 | 3.00 |
|---------------|------|------|------|------|------|------|------|------|------|------|------|
| 1.0 | 8.5 | 8.5 | 8.5 | 9.5 | 9.5 | 9.5 | 9.5 | 10.5 | 10.5 | 10.5 | 10.5 |
| 1.25 | 6.5 | 6.5 | 7.5 | 7.5 | 7.5 | 8.5 | 8.5 | 8.5 | 8.5 | 8.5 | 8.5 |
| 1.50 | 5.5 | 5.5 | 6.5 | 6.5 | 6.5 | 6.5 | 6.5 | 7.5 | 7.5 | 7.5 | 7.5 |
| 1.75 | 5.5 | 5.5 | 5.5 | 5.5 | 5.5 | 5.5 | 5.5 | 6.5 | 6.5 | 6.5 | 6.5 |
| 2.00 | 4.5 | 4.5 | 4.5 | 4.5 | 5.5 | 5.5 | 5.5 | 5.5 | 5.5 | 5.5 | 5.5 |
| 2.25 | 4.5 | 4.5 | 4.5 | 4.5 | 4.5 | 4.5 | 4.5 | 4.5 | 4.5 | 5.5 | 5.5 |
| 2.50 | 3.5 | 3.5 | 3.5 | 4.5 | 4.5 | 4.5 | 4.5 | 4.5 | 4.5 | 4.5 | 4.5 |
| 2.75 | 3.5 | 3.5 | 3.5 | 3.5 | 3.5 | 3.5 | 4.5 | 4.5 | 4.5 | 4.5 | 4.5 |
| 3.00 | 3.5 | 3.5 | 3.5 | 3.5 | 3.5 | 3.5 | 3.5 | 3.5 | 3.5 | 3.5 | 4.5 |

TABLE 3 CALCULATED DCR

| w (mm)\r (mm) | 1.00 | 1.20 | 1.40 | 1.60 | 1.80 | 2.00 | 2.20 | 2.40 | 2.60 | 2.80 | 3.00 |
|---------------|------|------|------|------|------|------|------|-------|-------|-------|-------|
| 1.0 | 46.3 | 41.1 | 37.5 | 72.3 | 67.8 | 64.2 | 61.3 | 215.8 | 208.2 | 201.8 | 196.2 |
| 1.25 | 17.5 | 15.5 | 23.9 | 22.0 | 20.5 | 19.3 | 33.0 | 31.5 | 30.3 | 29.2 | 28.3 |
| 1.50 | 11.7 | 10.3 | 15.8 | 14.4 | 13.4 | 12.5 | 11.8 | 11.3 | 18.5 | 17.8 | 17.2 |
| 1.75 | 13.2 | 11.5 | 10.3 | 9.4 | 8.6 | 8.1 | 7.6 | 12.3 | 11.8 | 11.3 | 10.9 |
| 2.00 | 8.3 | 7.2 | 6.4 | 5.8 | 9.5 | 8.8 | 8.3 | 7.8 | 7.5 | 7.1 | 6.9 |
| 2.25 | 9.1 | 7.9 | 7.0 | 6.3 | 5.8 | 5.4 | 5.1 | 4.8 | 4.5 | 7.7 | 7.3 |
| 2.50 | 5.2 | 4.5 | 4.0 | 6.9 | 6.3 | 5.8 | 5.4 | 5.1 | 4.9 | 4.6 | 4.4 |
| 2.75 | 5.7 | 4.9 | 4.3 | 3.9 | 3.5 | 3.3 | 5.8 | 5.5 | 5.2 | 4.9 | 4.7 |
| 3.00 | 6.1 | 5.2 | 4.6 | 4.1 | 3.8 | 3.5 | 3.2 | 3.1 | 2.9 | 2.7 | 5.0 |

TABLE 3 lists the calculated DCR values obtained through (6). The DCR value increases with the reduction of internal radius r and the increase of the number of turns. When $r = 1.0$, 1.5mm, the DCR are much higher than other cases, so they are excluded from the candidates. The left solutions have the number of turns 3.5, 4.5, 5.5, 6.5. Those four winding solutions will be put into simulation to do further analysis.

The number of turns is obtained through (5) by assuming that the total inductance value is 1 μ H. However, it is only used to calculate the rough number of turns. The inductor designed with the parameters in the calculation might not get the assumed inductance value. This is because (5), which uses the calculated inductance value of closed magnetic path with constrained regular effective area A_e such as E I ferrite magnetic cores, can introduce some error in inductance calculation. The proposed inductor does not have constant effective area A_e along the magnetic path. The equivalent length of magnetic path could also contribute some error. A FEA simulation for each number of turns is executed to further get the right parameters for designing the inductance value. Figure 5 and Figure 6 show the simulated inductance value and DCR for different number of turns. For all the cases, the inductance value has the trend of increase with the increase of radius while it has the trend of decrease with the increase of the coil width. The outer diameter expressed in (7) is limited by the width of the magnetic core 9mm which means $r + w$ should be less than 4.5mm in the simulation. Therefore, in Figure 5 and Figure 6, the maximum radius varies for different values of coil width.

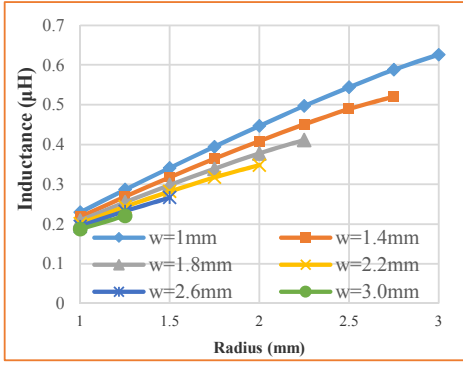
$$d = 2(w + r) \quad (7)$$

In practice, more restrictions are added to leave some margin at both sides of terminals. DCR of the inductor has the same trend as inductance. It increases with increase of the radius r and reduces with increases of coil width w . Therefore, the design of such an inductor is essentially choosing the right parameters to reduce DCR while achieving the expected inductance value. For the 3.5 turn design, DCR is very small since it has less number of turns and thicker copper for each turn, but the inductance value is not high enough to meet the requirement of 1 μ H specification. It can be excluded from the comparison, then only 4.5 turn, 5.5 turn, 6.5 turn are further considered as candidates. For the 4.5 turn design, the maximum inductance value can be higher than 1 μ H, it is at about $r=2.75$ mm, $w=1$ mm. There are some points, which are not shown in the curves, reaching 1 μ H point. For example, $r=2.85$, $w=1.1$ mm, they are very similar to the point $r=2.75$ mm, $w=1$ mm. For 5.5 turn design, there are three combinations. $r=1.8$ mm, $w=1$ mm; $r=2$ mm, $w=1.4$ mm; $r=2.25$, $w=1.8$. For 6.5 turn design, there are five candidates. $r=1.2$ mm, $w=1$ mm; $r=1.3$ mm, $w=1.4$ mm; $r=1.4$ mm, $w=1.8$ mm; $r=1.45$ mm, $w=2.2$ mm; $r=1.5$ mm, $w=2.6$ mm. For different groups of parameters, the DCR shown in Figure 6 is different.

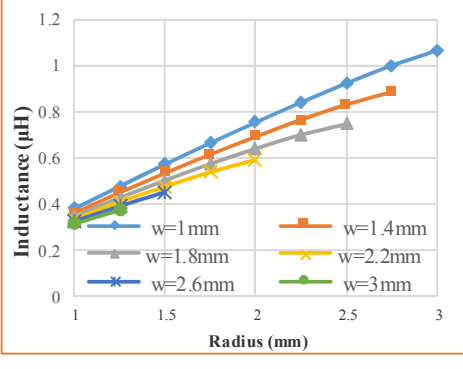
Since the design of an inductor is essentially finding the trade off point of the inductance and DCR under the certain volume condition, it is hard to determine through either the inductance value curves or the DCR value curves. A new

TABLE 4 SIMULATION RESULTS FOR SELECTED CANDIDATES

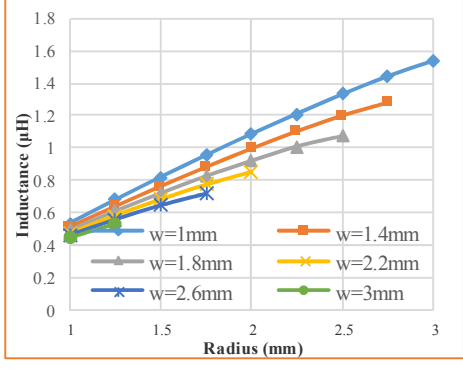
| No. | 1 | 2 | 3 | 4 | 5 | 6 | 7 | 8 | 9 |
|------------------------------|-------|-------|-------|------|-------|-------|-------|-------|-------|
| Turns | 4.5 | 5.5 | 5.5 | 5.5 | 6.5 | 6.5 | 6.5 | 6.5 | 6.5 |
| Radius (mm) | 2.75 | 1.8 | 2 | 2.25 | 1.2 | 1.3 | 1.4 | 1.45 | 1.5 |
| Width (mm) | 1 | 1 | 1.4 | 1.8 | 1 | 1.4 | 1.8 | 2.2 | 2.6 |
| r + w (mm) | 3.75 | 2.8 | 3.4 | 4.05 | 2.2 | 2.7 | 3.2 | 3.65 | 4.1 |
| DCR (m Ω) | 10.5 | 10.8 | 9.28 | 8.4 | 15 | 12.5 | 11.3 | 9.52 | 9.5 |
| L/DCR (μ H/m Ω) | 0.095 | 0.088 | 0.107 | 0.12 | 0.068 | 0.080 | 0.093 | 0.098 | 0.103 |



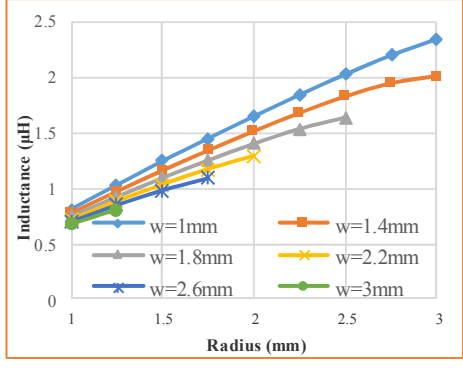
(a) N=3.5



(b) N=4.5



(c) N=5.5



(d) N=6.5

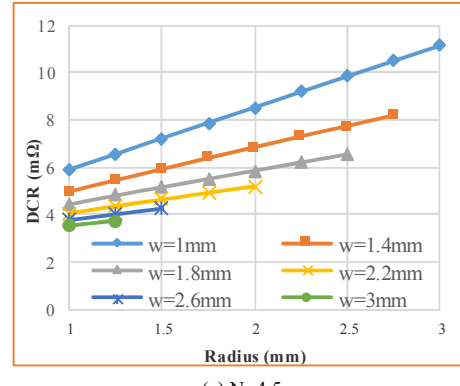
Figure 5. Inductance vs Radius with coil width as a parameter.

parameter L/R is defined in this paper as a new criterial to choose and optimize the design. It should be noted that this parameter is different from the quality factor $\omega L/R$ which also reflects the AC performance of the magnetics. It is mainly used to show the low frequency characteristics of an inductor. Figure 7 shows the curves of L/R for number of turns 4.5, 5.5, 6.5. It can be observed that the L/R is higher for $N=5.5$ than the other two numbers of turns for the same radius and coil and L/R of the selected candidates.

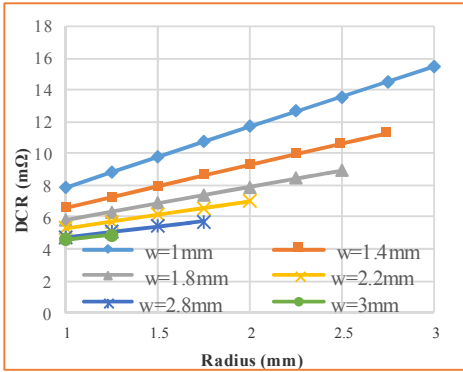
In TABLE 4, No. 4 ($N=5.5$, $r=2.25\text{mm}$, $w=1.8\text{mm}$) has the lowest DCR and the highest L/R . However, the $r + w$ value is 4.05 which is close to half width of the module. In the real practice of manufacture, by considering the mechanical stress of the magnetic material when bending the coil terminals, there should be 3mm margin (1.5mm on both sides), which means $r + w \leq 3\text{mm}$. With this restriction applied to the candidates, three options are left. They are No. 2 ($N=5.5$, $r=1.8\text{mm}$, $w=1\text{mm}$), No. 5 ($N=6.5$, $r=1.2\text{mm}$, $w=1\text{mm}$) and No. 6 ($N=6.5$, $r=1.3\text{mm}$, $w=1.4\text{mm}$). No. 2 has the highest L/R value and it can be selected as a final design. Since the $r + w$ value for No. 2 is 2.8mm, w can be further increased by 0.2mm ($r + w$ is not larger than 3mm) which will not lead to significant decrease of the inductance value. And prototypes will be made based on this parameters ($N=5.5$, $r=1.8\text{mm}$, $w=1.2\text{mm}$). A new simulation is executed based on the selected parameters. The inductance value at no load is $1.1\mu\text{H}$, it drops to $1.01\mu\text{H}$ which still satisfies the specification. A field distribution of flux density at 6A current excitation in the designed inductor is shown in Figure 8. The maximum flux density happens around the winding, which is 0.24mT . The saturation flux density of the magnetic materials is about 1T . Therefore, the inductor still has the potential to be used in higher output current application, such as 12V input, 5V/8A output power module.

IV. PROTOTYPE AND EXPERIMENT

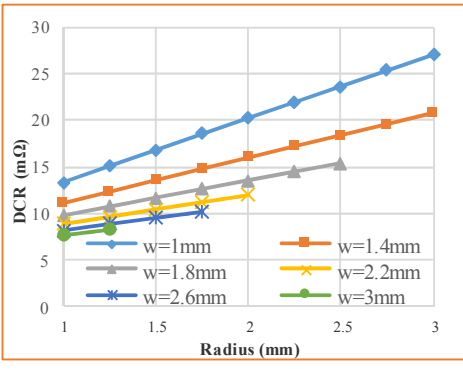
In this section, inductor prototype will be made with the parameters obtained in the last section. Figure 9(a) and Figure 9(b) show the top view and bottom view of the inductor. Two leads were extended from the winding and bended at the bottom of the inductor for soldering on the small PCB board



(a) N=4.5

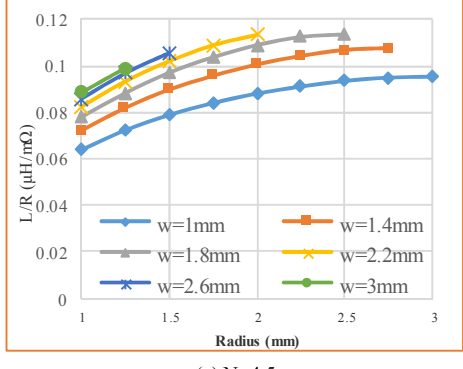


(b) N=5.5

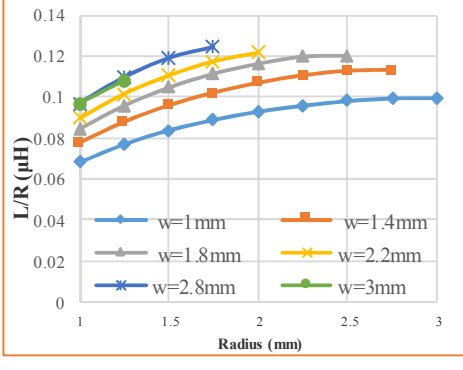


(c) N=6.5

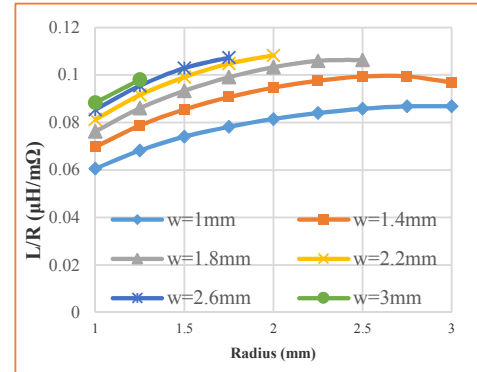
Figure 6. DCR vs Radius with coil width as a parameter.



(a) N=4.5



(b) N=5.5



(c) N=6.5

Figure 7. L/R vs Radius with coil width as a parameter.

which is 0.4mm thick. Discrete components, such as regulator and resistors in the power circuit, are soldered on the area of PCB board underneath the cavity of the inductor. Red glue is used at the bottom of the magnetic core where winding is embedded and the ceiling of the cavity where the regulator chip is located to strengthen the adhesive force during the assembling process. Figure 9(c) shows the bottom view of the assembled power module. Before assembling the inductor on the PCB, inductance vs DC bias is measured using a Wayne Kerr 3260B LCR meter. With the purpose of comparison, it is also simulated through FEA simulation. Figure 10 shows the test and simulation results. They correlate with each other very well. Figure 11 shows the resistance versus switching frequency by measurement and simulation. The power module is then soldered on an evaluation board to do loss analysis and performances test. Loss characteristic of the magnetic material is firstly teste to obtain the parameters of Stenmez equations used in FEA simulation and calculate the core loss. Figure 12 shows the power loss the magnetic materials versus flux density with frequency as a parameter. With the simulated core loss, loss breakdown of the power module is executed. Figure 13 shows the loss of the inductor and the switches.

Two comparison experimental tests will be done with the assembled power module to verify its performance. The first one is to show the advantage of the proposed packaging technology over the conventional plastic packing technology by using the same PCB and circuit but different inductors and packaging. The second one is to compare the performances of the proposed power module with the state-of-art plastic packaging power modules in industry.

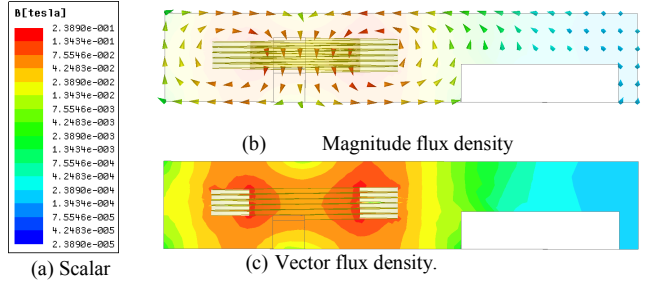


Figure 8. Simulated flux distribution.

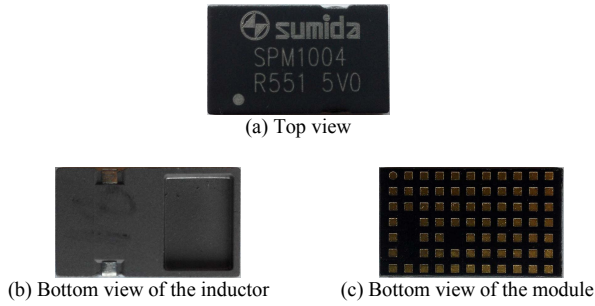
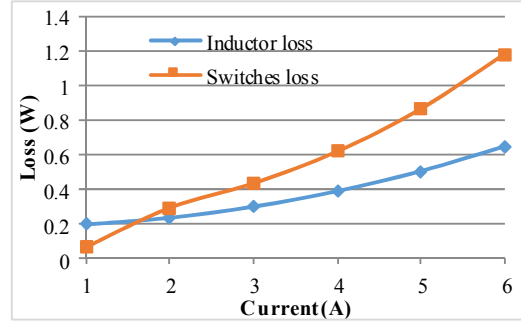


Figure 9. Picture of the power module.



(a) Inductor loss and switches loss.

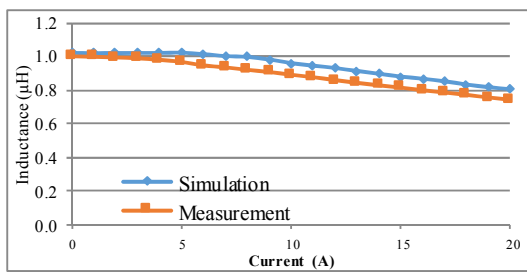


Figure 10. Inductance value of the proposed inductor via DC bias.

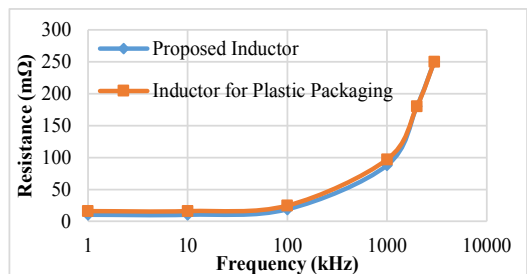


Figure 11. Resistance vs frequency.

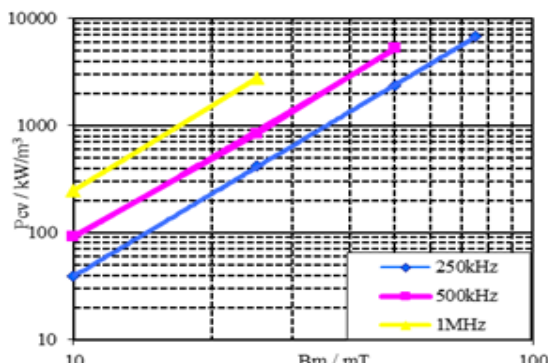
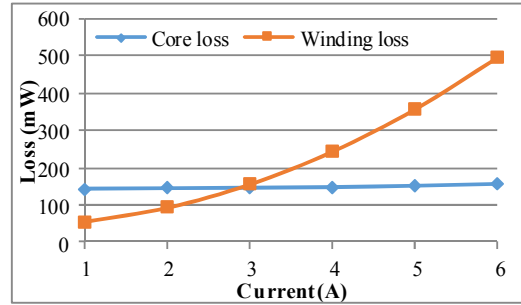


Figure 12. Loss characteristic of the magnetic material.



(a) Winding loss and core loss.

Figure 13. Loss breakdown of the power module.

As described in Section I, one of the advantages of the proposed power module is that it is able to have larger volume of inductor than that in conventional plastic packaging which has to leave enough margin for injecting plastic material during packaging process. For inductors made with the same magnetic material, larger volume means higher inductance value or lower DCR. Figure 14 shows the picture of the selected metal powder composite inductor used for plastic packaged module. The volume of the inductor is $6\text{mm} \times 6\text{mm} \times 2.2\text{mm}$. It has $0.9\mu\text{H}$ inductance value and $17\text{m}\Omega$ DCR. Figure 15 shows its inductance value versus DC bias. The prototype of the proposed inductor has $1\mu\text{H}$ inductance value and $11\text{m}\Omega$ DCR. The inductor for plastic packaging has much smaller saturation current than the proposed inductor because it has smaller volume and thinner wire. Both inductors are soldered on the same PCB board to test their efficiency performances under the same load conditions. Figure 16 shows the small board with inductor soldered on it. Figure 17 shows the efficiency comparison results. It can be observed that the PCB board with the proposed inductor has about 2% higher efficiency across the whole load range since it has lower DCR and better performances.



Figure 14. Selected metal powder composite inductor for plastic packaging.

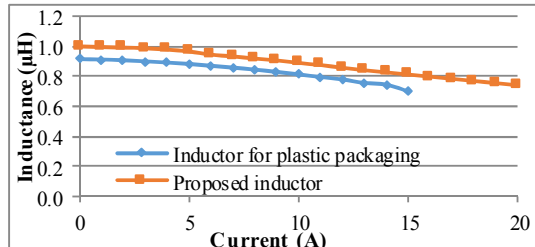


Figure 15. Inductance of the proposed inductor and the selected inductor for plastic packaging.

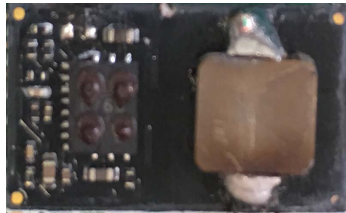


Figure 16. PCB of the power module with selected metal powder composite inductor.

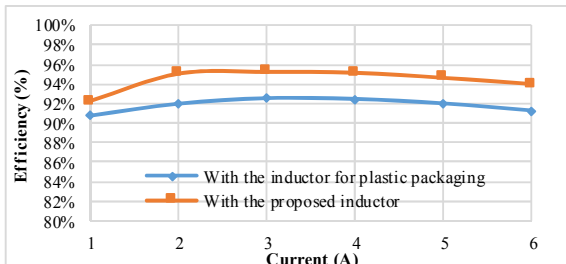


Figure 17. Efficiency curves of the power modules with different inductors.

V. CONCLUSION

The special magnetic component proposed in this paper has functions of both inductor and the packaging. A PSI² structured power module is designed to show the benefit of the magnetic component. Compared with plastic packaging solution, the proposed design has larger inductor volume, and thus higher inductance value. Experimental test shows that the designed power module has a 95.2% high peak efficiency and high saturation current.

REFERENCES

- [1] E. Waffenschmidt; B. Ackermann; and J. A. Ferreira, "Design method and material technologies for passives in printed circuit board embedded circuits," *IEEE Trans. Power Electron.*, vol. 20, no. 3, pp. 576–584, May 2005.
- [2] M. H. Lim; J. D. van Wyk; and F. C. Lee, "Hybrid integration of a low voltage, high-current power supply buck converter with an LTCC substrate inductor," *IEEE Trans. Power Electron.*, vol. 25, no. 9, pp. 2287–2298, Sep. 2010.
- [3] Qiang Li; Yan Dong; F.C.Lee; Gilham, D., "High-Density Low-Profile Coupled Inductor Design for Integrated Point-of-Load Converters," in *Power Electronics, IEEE Transactions on*, vol.28, no.1, pp.547-554, Jan. 2013.
- [4] Laili Wang; Yunqing Pei; Xu Yang; Zhaoan Wang, "Design of Ultrathin LTCC Coupled Inductors for Compact DC/DC Converters," in *Power Electronics, IEEE Transactions on*, vol.26, no.9, pp.2528-2541, Sept. 2011.
- [5] Mino, M.; Yachi, T.; Tago, Akio; Yanagisawa, Keiichi; Sakakibara, K., "A new planar microtransformer for use in micro-switching converters," in *Magnetics, IEEE Transactions on*, vol.28, no.4, pp.1969-1973, Jul 1992.
- [6] Yun, Eui-Jung; Jung, Myunghlee; Chae Il Cheon; Hyoung Gin Nam, "Microfabrication and characteristics of low-power high-performance magnetic thin-film transformers," in *Magnetics, IEEE Transactions on*, vol.40, no.1, pp.65-70, Jan. 2004.
- [7] Kowase, I.; Sato, T.; Yamasawa, K.; Miura, Y., "A planar inductor using Mn-Zn ferrite/polyimide composite thick film for low-Voltage and large-current DC-DC converter," in *Magnetics, IEEE Transactions on*, vol.41, no.10, pp.3991-3993, Oct. 2005.
- [8] Laili Wang; Yunqing Pei; Xu Yang; Yang Qin; Zhaoan Wang, "Improving Light and Intermediate Load Efficiencies of Buck Converters With Planar Nonlinear Inductors and Variable On Time Control," in *Power Electronics, IEEE Transactions on*, vol.27, no.1, pp.342-353, Jan. 2012.
- [9] Lim, M.H.F.; van Wyk, J.D.; Zhenxian Liang, "Internal Geometry Variation of LTCC Inductors to Improve Light-Load Efficiency of DC-DC Converters," in *Components and Packaging Technologies, IEEE Transactions on*, vol.32, no.1, pp.3-11, March 2009.
- [10] Lim, M.H.; van Wyk, J.D.; Lee, F.C.; Ngo, K.D.T., "A Class of Ceramic-Based Chip Inductors for Hybrid Integration in Power Supplies," in *Power Electronics, IEEE Transactions on*, vol.23, no.3, pp.1556-1564, May 2008.
- [11] Hahn, R.; Krumbholz, S.; Reichl, H., "Low profile power inductors based on ferromagnetic LTCC technology," in *Electronic Components and Technology Conference, 2006. Proceedings. 56th*, vol., no., pp. 528–533.
- [12] Mingkai Mu; Yipeng Su; Qiang Li; Lee, F.C., "Magnetic characterization of low temperature co-fired ceramic (LTCC) ferrite materials for high frequency power converters," in *Energy Conversion Congress and Exposition (ECCE), 2011 IEEE*, vol., no., pp.2133-2138, 17-22 Sept. 2011.
- [13] Yipeng Su; Qiang Li; Mingkai Mu; Gilham, D.; Reusch, D.; Lee, F.C., "Low profile LTCC inductor substrate for multi-MHz integrated POL converter," in *Applied Power Electronics Conference and Exposition (APEC), 2012 Twenty-Seventh Annual IEEE*, vol., no., pp.1331-1337, 5-9 Feb. 2012.
- [14] Qiang Li; Lee, F.C., "High Inductance Density Low-Profile Inductor Structure for Integrated Point-of-Load Converter," in *Applied Power Electronics Conference and Exposition, 2009. APEC 2009. Twenty-Fourth Annual IEEE*, vol., no., pp.1011-1017, 15-19 Feb. 2009.
- [15] Yipeng Su; Qiang Li; Lee, F.C., "Design and Evaluation of a High-Frequency LTCC Inductor Substrate for a Three-Dimensional Integrated DC/DC Converter," in *Power Electronics, IEEE Transactions on*, vol.28, no.9, pp.4354-4364, Sept. 2013.
- [16] Lopera, J.M.; Prieto, M.J.; Pernia, A.M.; Nuno, F., "A multiwinding modeling method for high frequency transformers and inductors," in *Power Electronics, IEEE Transactions on*, vol.18, no.3, pp.896-906, May 2003.
- [17] Jizheng Qiu; Sullivan, C.R., "Design and Fabrication of VHF Tapped Power Inductors Using Nanogranular Magnetic Films," in *Power Electronics, IEEE Transactions on*, vol.27, no.12, pp.4965-4975, Dec. 2012.
- [18] Jian Lu; Hongwei Jia; Xuexin Wang; Padmanabhan, K.; Hurley, W.G.; Shen, Z.J., "Modeling, Design, and Characterization of Multiturn Bondwire Inductors With Ferrite Epoxy Glob Cores for Power Supply System-on-Chip or System-in-Package Applications," in *Power Electronics, IEEE Transactions on*, vol.25, no.8, pp.2010-2017, Aug. 2010.